Critical behavior of the uniaxial ferromagnetic monolayer Fe(110) on W(110)

Hans-Joachim Elmers, Jens Hauschild, and Ulrich Gradmann*
Physikalisches Institut, Technische Universität Clausthal, D-38678 Clausthal-Zellerfeld, Germany
(Received 11 July 1996)

The critical behavior of a ferromagnetic monolayer has been investigated experimentally for the case of the thermodynamically stable pseudomorphic monolayer Fe(110) on W(110). The nearly ideal monolayer samples were composed of monolayer Fe(110) stripes, grown by step flow from the atomic steps of the W(110) substrate, with a distribution of stripe widths around a mean value of 40 nm, and virtually infinite length. The magnetic properties were measured by spin-polarized low-energy electron diffraction, which could be done in weak magnetic fields up to 2 Oe. The monolayer samples show uniaxial magnetic anisotropy with the easy axis [110] in the film plane. Magnetization tails above T_c were shown to be a result of convolution of the critical power law with the monolayer stripe width distribution. Using an appropriate deconvolution, critical power laws could be established for both magnetization M and susceptibility χ, with critical exponents $\beta=(0.134 \pm 0.003)$ and $\gamma=(2.8\pm0.2)$, corresponding to predictions of a two-dimensional anisotropic Heisenberg model. [S0163-1829(96)03145-1]

I. INTRODUCTION

The magnetic phase transition in a two-dimensional (2D) lattice is a playground for fundamental theoretical models of phase transitions. Differences of the observable properties borne out by these models are more pronounced in 2D than in 3D systems, and both analytical and numerical treatment is typically easier for reduced dimensionality. The situation is the opposite in experiment. The preparation of a true ferromagnetic monolayer, which corresponds to those 2D models, is far more difficult and problematic than that of a 3D crystal, and the measurement of its magnetic properties requires advanced techniques of outstanding sensitivity. In the present paper, we report on the critical behavior of the best available experimental approach to the ferromagnetic monolayer, given by the pseudomorphic monolayer Fe(110) on W(110). The magnetic properties were measured by spin-polarized low-energy electron diffraction (SPLEED).

The nature of the 2D magnetic phase transition is governed by magnetic anisotropies. This is shown most clearly by two limiting cases. In the limit of infinite uniaxial anisotropy, represented by the 2D Ising model, the exact Onsager solution[1,2] shows a second-order phase transition with critical exponents $\beta=1/8$ and $\gamma=7/4$ for magnetization and susceptibility, respectively. In the isotropic limit instead, for the case of the isotropic Heisenberg model with short-range interactions, no phase transition to a long-range-ordered phase is expected at all at finite temperatures.[3] These limiting cases gain a central role by the hypothesis of universality, formulated by Griffiths,[4] now widely accepted as a result of renormalization-group theory,[5] which states that the critical exponents and amplitudes are universal in the sense that they depend, for given dimensionality d ($d=2$ in our case), only on the number n of equivalent spin components and on the range of the exchange interactions. 2D magnetic systems with short-range exchange interactions then can be assigned, with respect to their critical behavior, to three universality classes. The case $n=2$ is represented by the planar or XY model, in which there is no conventional phase transition to an ordered state, but a ''Kosterlitz-Thouless'' phase transition[6,7] to a state of infinite correlation length without spontaneous long-range order. However, it has been shown recently[8] that finite-size XY systems, which are good models for real film structures, show a rounded phase transition with an effective exponent $\beta=0.23$. Because of the absence of a phase transition for $n=3$ (isotropic Heisenberg model), one then would expect, from these universality ideas, that 2D systems should show either Ising-like ($n=1$) or XY-like ($n=2$) critical behavior.[8] However, any real monolayer shows finite anisotropies and therefore should rather be described by anisotropic Heisenberg models.[9,10]

The phase transition in a real system becomes much more complicated if long-range magnetostatic interactions play an essential role. This is the case if the surface type crystalline anisotropy has the film normal as an easy axis and therefore competes with the magnetostatic interactions, which show up as shape anisotropy supporting in-plane magnetization. For a theoretical discussion of the rich variety of critical phenomena in those perpendicularly magnetized films see Ref. 11 and references given there. Those complications in uniaxial 2D systems caused by competition of crystalline and shape anisotropy are avoided if the easy axis is in-plane. This is the case for our system Fe(110) on W(110), which therefore shows a much clearer relation to elementary models of 2D magnetism than perpendicularly magnetized films.

Early attempts to experimentally realize 2D magnetic systems used layered crystals like K_2NiF_4 or related compounds.[12,13] In order to minimize 3D interactions between the 2D magnetically ordering sheets, the investigations were preferentially carried out for 2D antiferromagnets, which are equivalent to the ferromagnets with respect to their critical behavior. Even then, the experimentally determined values of β, for uniaxial systems, were typically $\geqslant 0.14$, near but definitely larger than the Ising value 0.125. Supposedly, the difference was connected with residual 3D interactions.

To get rid of these 3D interactions, true single magnetic monolayers are required. Ultrathin magnetic films in the monolayer regime can now be prepared by modern epitaxial techniques in UHV.[14,15] However, true monolayers are rare. As model systems with uniaxial anisotropy, it seemed inter-

esting at first glance to investigate perpendicularly magnetized films, like Fe(100) films on Cu(100),[16] on Pd(100),[17] and on Ag(100).[18] The critical behavior of the magnetization was measured and Ising-like exponents have been reported for those systems. Their evaluation however was severely complicated by magnetization tails which extended over 3–5 % above T_C. These tails were explained as finite-size effects.[17–20] However, deviations from layer-by-layer-growth and the competition between perpendicular crystalline and easy-plane shape anisotropy may have contributed to the tails in these perpendicularly magnetized films, too. The competition of surface and shape anisotropy is avoided in films with in-plane uniaxial anisotropy like Fe on Ag(111) (Ref. 21), and Ni on W(110),[22] where Ising-like values for β have been reported for films consisting of 2–4 monolayers, and the tails were reduced to the order of 1%.

For a true magnetic monolayer with an in-plane easy axis, a unique candidate is given by Fe(110) on W(110). Because the surface energy of Fe is lower than that of W, the monolayer is thermodynamically stable.[23] Because both metals are bcc, and the misfit is moderate ($f_{\mathrm{FeW}}=-9.4\%$), the monolayer is pseudomorphic[24] and therefore shows the 2D translational symmetry of the W(110) substrate. This is different in films above the monolayer, e.g., in the films consisting of roughly 1.4 ML which show a Curie temperature near RT and therefore have been investigated recently in detail[25–27] but provide a system of double layer islands on a monolayer substrate rather than a true monolayer.[28] Magnetism in the Ag-covered monolayer W(110)/Fe(110)/Ag, which is magnetized in the plane, has been investigated previously by Mössbauer spectroscopy[29,30,23] and magnetometry.[31,23] The Ag-covered monolayer shows a uniaxial in-plane easy axis along [110] and a Curie temperature of 282 K. Like the Ag-covered monolayer, the uncovered one shows an in-plane easy axis [110], but combined with a lowered Curie temperature of 225 K.[32]

The present paper is concerned with the critical properties of this uncovered monolayer of Fe(110) on W(110). Both out-of-plane and in-plane surface type magnetic anisotropies of this monolayer are of the order of 0.3 mJ/m^2.[32] Corresponding to anisotropy fields of several Tesla, these anisotropies are strong in comparison with usual bulk magnetocrystalline anisotropies of Fe. Nevertheless, the anisotropy energies per atom of 0.11 meV/atom$=k_B$ 2 K (Ref. 32) are small in comparison with exchange energies of the order $k_B T_C$. The monolayer Fe(110) on W(110) therefore represents an anisotropic Heisenberg rather than an Ising model. Nevertheless 2D Ising critical behavior can be expected in a first approximation [a similar presentation of the double layer Fe(100) on W(100), which approaches 2D XY critical behavior, has been given elsewhere[33]]. Both the remanent magnetization and the susceptibility of the uncovered monolayer Fe(110) on W(110) were determined in the critical regime, using SPLEED. Part of the data has been published previously.[32,34–36] Because the transition in our samples is rather sharp, with a width of the tails of the order of 0.3% only, we previously analyzed the data using a single component power law, interpreting the tails as finite-size features.[9] This approximation is quite familiar in ultrathin film work,[17,18,25,37] but it is not free from arbitrarities, in particular with respect to the determination of critical exponents. In the present paper, we consider the fact that the films consist of monolayer stripes, grown by step flow from the atomic steps of the W substrate, with a distribution of stripe widths about a mean value of typically 40 nm.[32] By intentionally changing the width of these monolayer stripes, we will show that the magnetization tails are a result of convolution of the critical power law with the stripe width distribution. This correct interpretation of the tails enables a deconvolution of them and unambiguous determination of critical exponents. The aim of the present paper is a comprehensive presentation of experiments in the critical regime of the uncovered monolayer Fe(110) on W(110), including data on the nature of the magnetization tails and the corresponding evaluation of them. It will be shown that the critical exponents determined along those lines are independent of the width of the distribution and therefore can be taken as intrinsic properties of the ideal 2D limiting case.

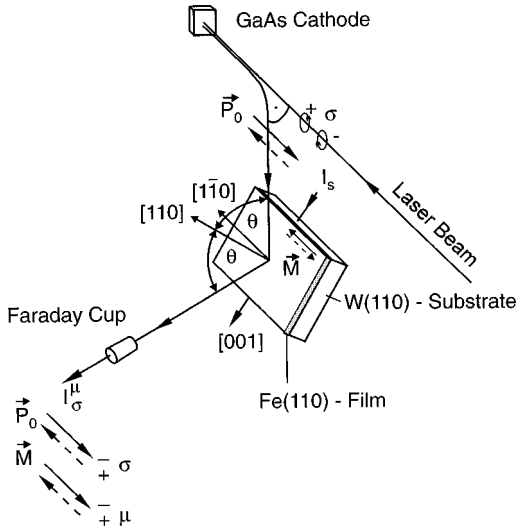

FIG. 1. Geometry of the SPLEED experiment.

II. EXPERIMENTAL

Fe was deposited on atomically clean W(110) surfaces at pressures below 10^{-10} Torr. The first monolayer grows in registry with the W(110) substrate, forming what is called a pseudomorphic monolayer, showing the 2D translational symmetry of the substrate.[24] For preparation, we used substrate temperatures of $T_p=660$ K in this study, for which the monolayer grows by step flow from the atomic steps of the substrate, as has been shown previously using scanning tunneling microscopy.[32] The film therefore is composed of monolayer stripes attached to the W terrace edges which were oriented arbitrarily on the surface. The average width W of terraces between atomic steps was of the order of 40 nm, as a rule, their length is virtually infinite.

SPLEED was performed by specular reflexion of spin-polarized electrons in a geometry as shown in Fig. 1. A GaAs photocathode is irradiated by circularly polarized light from a laser diode, resulting in a longitudinally spin-polarized electron beam with a polarization P_0 of the order of 20%. After a 90° electrostatic deflection, the electron beam becomes transversally polarized. This transversally polarized beam is reflected in the (110) scattering plane of the

W(110)/Fe(110) target. The polarization axis of the electron spin coincides with the normal of the scattering plane which in turn coincides with the easy axis [110] of the monolayer magnetization. An external magnetic field H up to 200 Oe can be applied along this axis. It is generated by a direct current I_s through the stripe-shaped W substrate. Because the field is constrained to the surroundings of the sample, the deflecting action on the reflected electrons is minimized, and SPLEED is possible using this technique in fields up to 2 Oe.[34]

Using a Faraday cup, we measure the specularly reflected intensities I_σ for both signs $\sigma=\pm 1$ of P_0. By conveniently modulating σ by optical methods, we measure the scattering asymmetries

$$P_0A=(I_+-I_-)/(I_++I_-). \tag{1}$$

Being uniaxial ultrathin films, our samples show in zero field, for given $T<T_C$, two degenerate single domain ground states with opposite sign $\mu=\pm 1$ of the magnetization. Our experimental method then is based on preparing those two single domain states, and to measure scattering asymmetries

$$P_0A^\mu=(I_+^\mu-I_-^\mu)/(I_+^\mu+I_-^\mu) \tag{2}$$

for both signs μ. The problem is that with the low magnetic fields available we can switch between the two states only in a range of some K below T_C, see Fig. 4, below, because the coercive field rapidly increases beyond our available fields with decreasing temperatures. In a typical run, the samples therefore were cooled down to 115 K in periodically repeated field pulses of 200 G of given sign μ. They thus were fed in the critical regime into the single domain state μ, in which they remained at lower temperatures. P_0A^μ was then measured, during slowly warming up (1 K/min) in zero field, as a function of temperature T, as shown, for example, in Fig. 2(a). The asymmetries were then decomposed as usual into a spin-orbit asymmetry

$$P_0A_{so}=P_0(A^++A^-)/2, \tag{3}$$

which is independent of the magnetization, and an exchange asymmetry

$$P_0A_{ex}=P_0(A^+-A^-)/2, \tag{4}$$

which changes its sign with μ. The exchange asymmetry P_0A_{ex} is our magnetic signal. As shown in Fig. 2(b), it vanishes at T_C, whereas A_{so} is continuous.

Note that because our measurements are restricted to low fields and (slowly) drifting temperatures, we are not able to measure the square loops which undoubtedly would be observed in sufficiently strong fields at constant temperatures. For the critical regime however, the equivalence of remanent and spontaneous magnetization, which is the only feature of interest for the present work, is confirmed by the susceptibility data discussed in Sec. III C, below, in particular by Fig. 9.

All experiments of this work were done with kinetic energies of 49 eV, for which P_0A_{so} shows a minimum. A scattering angle of $\theta=32°$ was used for which P_0A_{so} shows a minimum, see Fig. 3(a) P_0A_{ex} there shows a maximum, see Fig. 3(b). As seen in Fig. 3(b), the shape of P_0A_{ex} versus θ is independent of T. This justifies our use of P_0A_{ex} as a measure of magnetic order, proportional to the magnetization M, at least in the critical regime.[38]

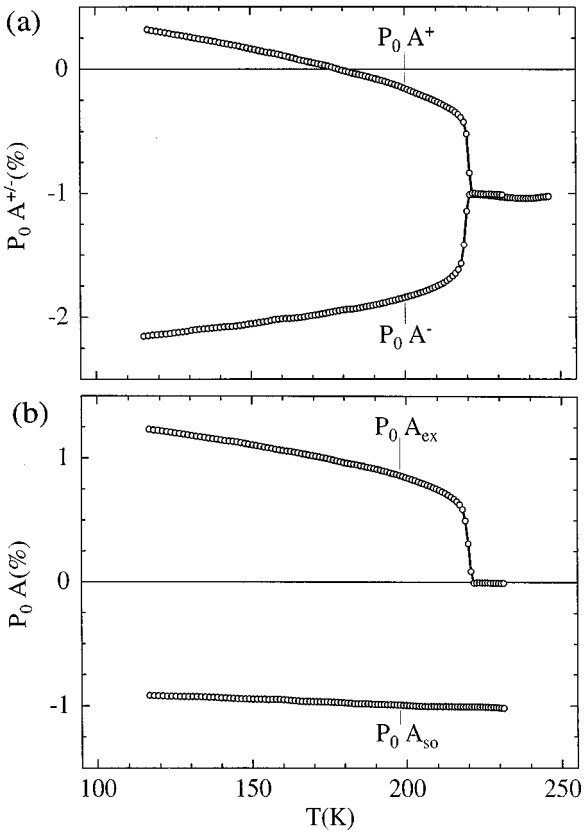

FIG. 2. Scattering asymmetries A versus temperature T for a film with coverage $\Theta=0.58$, prepared at 550 K. Because the electron-beam polarization P_0 is only roughly known (about 20%), the product P_0A is given which directly comes out of the measurement. (a) Asymmetries P_0A^+ and P_0A^- for positive and negative sign μ of the magnetization, respectively. (b) Exchange asymmetry $P_0A_{ex}=P_0(A^+-A^-)/2$ and spin-orbit asymmetry $P_0A_{so}=P_0(A^++A^-)/2$, respectively.

Different modes of data acquisition were used for magnetization and susceptibility, respectively. For measuring the (remanent) magnetization M, we used the fact that A_{so} can be considered as constant, in the critical regime, see Fig. 2(b), and therefore can be taken from the regime $T>T_C$. Because the residual laboratory field was negative ($H_{lab}=-40$ mOe), we measured as a rule $P_0A^-(T)$ only, in this residual field, with drifting temperatures after cooling down in pulsed (negative) fields, and took

$$P_0A_{ex}=-P_0A^-+P_0A_{so}/2 \tag{5}$$

as a measure for M. The measuring mode for the susceptibility was discussed in detail elsewhere.[34] In short, we again first created a single domain state μ by pulsed field cooling to 115 K. During warming up, we then measured asymmetries $A(H)$ in magnetic fields of constant magnitude H, with periodically changing sign. The result is shown in Fig. 4 for an example with $H=\pm 1.72$ Oe. For $T<220$ K, both $A(+1.72\text{ Oe})$ and $A(-1.72\text{ Oe})$ equal A^- (cooling in negative fields), because the coercive field is larger than H in

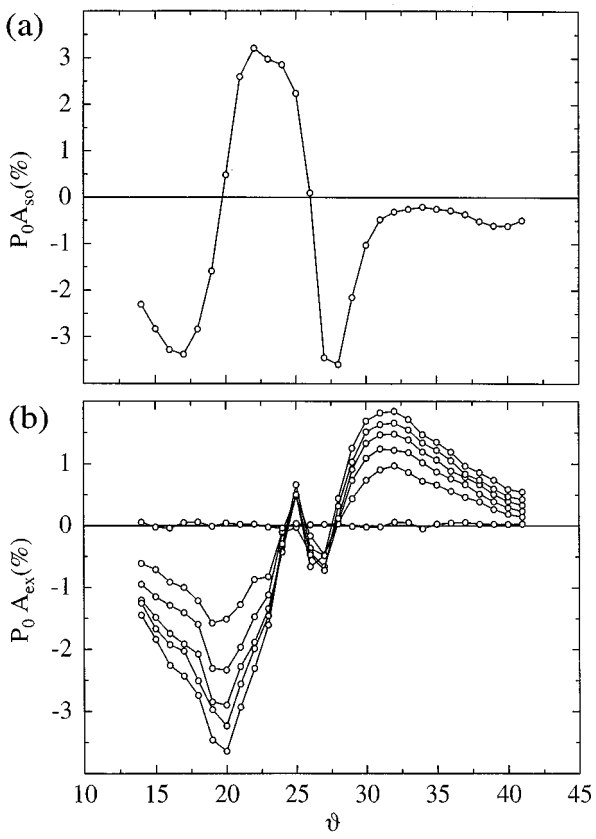

FIG. 3. Rocking curves of (a) P_0A_{so} and (b) P_0A_{ex} versus scattering angle Θ. The data in (b) were taken in zero field, with slowly rising temperatures, between 115 and 240 K, with a temperature increase of roughly 10 K during one run and further 10 K between two runs.

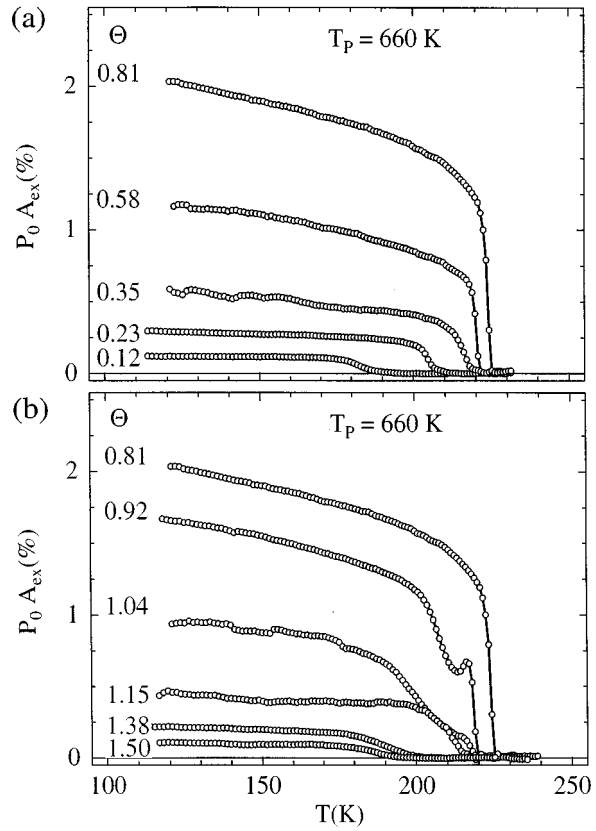

FIG. 5. (a) Exchange asymmetry P_0A_{ex} versus temperature T for partial monolayers with coverage $\Theta \leqslant 0.81$, prepared at 660 K. (b) As (a), but for $\Theta \geqslant 0.81$. Because the magnetization state is nonuniform in this regime, $P_0A_{ex} = -P_0A(-0.04\ \text{Oe}) + P_0A_{so}/2$ is not a true exchange asymmetry in the sense of Eq. (4).

this temperature range. $A(+1.72\ \text{Oe})$ and $A(-1.72\ \text{Oe})$ are shifted by a constant value which is caused by the deflection of the electrons by H. Near 220 K, the coercive field decreases to 1.72 Oe, and $A(+1.72\ \text{Oe})$ switches to A^+ for $T > 220$ K. Only in this temperature range, it then becomes possible to determine $A_{ex}(H,T)$ using Eq. (4), to be analyzed in terms of susceptibility as discussed below.

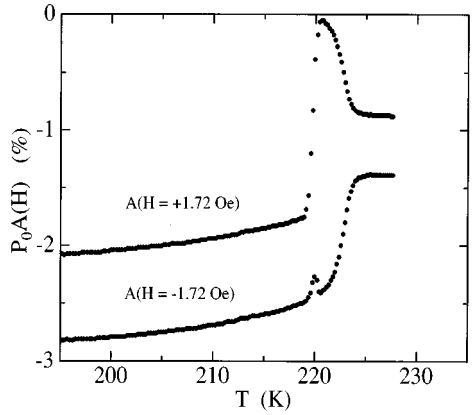

FIG. 4. Asymmetries $P_0A(H)$ versus temperature T, taken in periodically switched fields $H = \pm 1.72$ Oe during warming up after field cooling in -200 Oe. The shift of the curves below 220 and above 225 K is caused by minor deflections of the electron beam in the magnetic field.

III. RESULTS

Our analysis of the monolayer is based on samples with incomplete monolayer coverage $\Theta = 0.8$, which turned out as an optimum approximation of the true monolayer. This choice is explained in Sec. III A. Data on magnetization and susceptibility are presented in Secs. III B and III C, respectively.

A. The choice of $\Theta = 0.8$

In order to explain the choice of $\Theta = 0.8$, we present in Figs. 5(a) and 5(b) experimental data on P_0A_{ex} versus T for different coverages between 0.12 and 1.50 monolayers (ML). Data were taken usually in a residual field of -0.04 Oe after field cooling in -200 Oe pulses as described on Sec. II, above. The results for $0.12 \leqslant \Theta \leqslant 0.81$, presented in Fig. 5(a), are reasonable. As discussed in detail elsewhere,[32] the data represent the magnetization in monolayer stripes of variable (mean) width $w = \Theta W$, where $W = 40$ nm is the (mean) width of the W(110) terraces. The Curie temperature $T_C(w)$ follows a scaling law

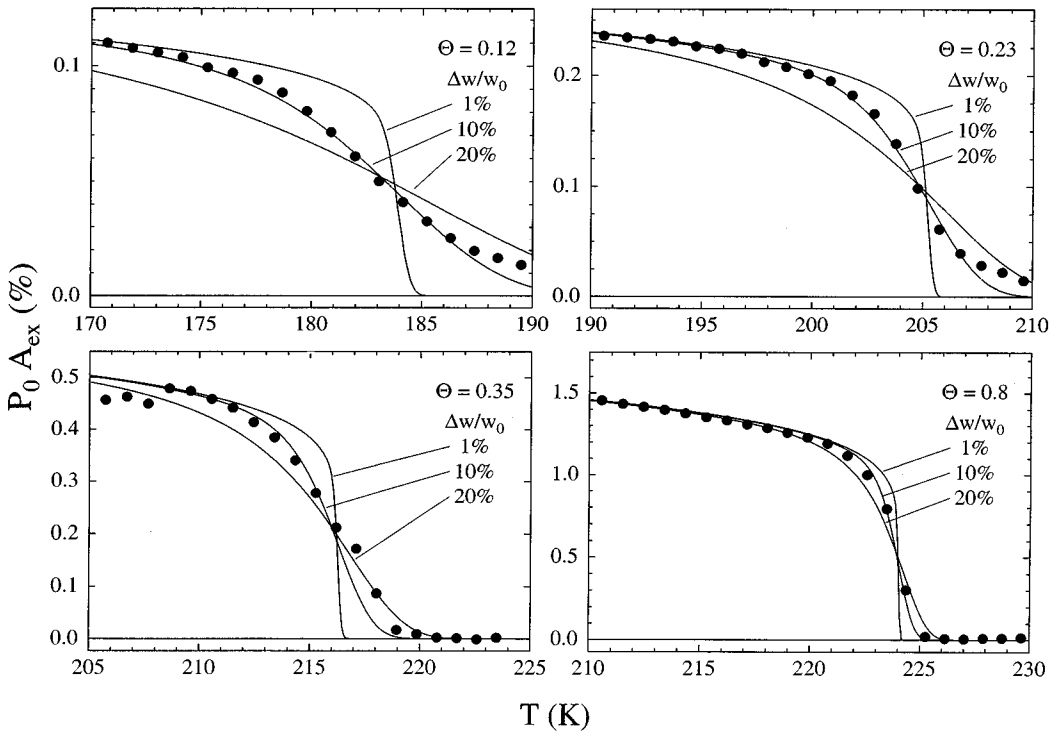

FIG. 6. Exchange asymmetry P_0A_{ex} versus temperature T in the critical range, for partial monolayers of different coverage Θ. Simulations as discussed in the main text, based on relative standard deviations $\Delta w/w_0$ of the monolayer stripe width distribution, as indicated.

$$[T_C(\mathrm{ML})-T_C(w)]/T_C(\mathrm{ML})=w_0/w \tag{6}$$

with $w_0=0.8$ nm and $T_C(\mathrm{ML})=230$ K, the latter being the Curie temperature of the extended monolayer, the stripe of infinite width. We observe in Fig. 5(a) that the transition is quite sharp for $\Theta=0.81$, but becomes wider for decreasing Θ. This is reasonable if some distribution is considered for the terrace width W of the W substrate. If we assume that Fe atoms condense on the terraces on which they stick, a distribution of W results in a similar distribution of w. This in turn induces some distribution of T_C which widens with decreasing Θ because of the increasing slope dT_C/dw [see Eq. (6)]. We can even make this idea quantitative in assuming a Gaussian distribution for W, with a standard deviation ΔW. The distribution of the stripe width then has a standard deviation

$$\Delta w=(\Delta W/W)w. \tag{7}$$

By Eq. (6), this results in a Gaussian distribution for T_C with a standard deviation

$$\Delta T_C=(\Delta W/W)(w_0/w)T_C(w). \tag{8}$$

The observed profile $A_{ex}(T)$ is then calculated by convolution of this T_C distribution with a power law $A_{ex}=\mathrm{const}[T_C-T]^{\beta}$. Figure 6 shows a simulation of the critical regimes along these lines for different values of Θ, using common values $\Delta W/W=\Delta w/w=10\%$ and $\beta=1/8$. The quite different slopes of the transitions for four different values of Θ are reproduced quite well.

The data for $\Theta>0.8$, shown in Fig. 5(b), do not fit in this bare monolayer scheme. Surprisingly, both $T_C(\Theta)$ and the saturation value of A_{ex} now decrease with increasing Θ. We guess that this is an indication of something like an antiferromagnetic coupling between different components, related to the frustration phenomena which we observed in films with $1.2<\Theta<1.5$, prepared at 300 K.[28] Of particular interest is the case $\Theta=0.92$ and the cusp of A just below T_C. It looks like the result of some partial antiferromagnetic compensation, below the cusp, which is overcome by the residual external field immediately below T_C. These explanations of the anomalies of course are highly speculative and definitely deserve further work. Independently of the true explanation which hopefully will come out from this forthcoming work, those anomalies prevent the use of films with $\Theta>0.85$ and justify our choice of $\Theta=0.8$ for monolayer investigation. Note that those stripes with $\Theta=0.8$ consist of roughly 200 atomic chains, with virtually infinite length. This is perhaps not a bad approximation to the ideal extended monolayer.

B. Magnetization

The discussion of the last section shows that the experimental data in the critical regime depend on the width of the distribution of terrace widths in the W(110) substrate, hence of stripe width and Curie temperature. For a high-resolution and high precision analysis of the critical behavior of the monolayer magnetization, we used two samples, both with $\Theta=0.8$, but with different widths of the distribution. Sample I was prepared on the same standard W-substrate area as the

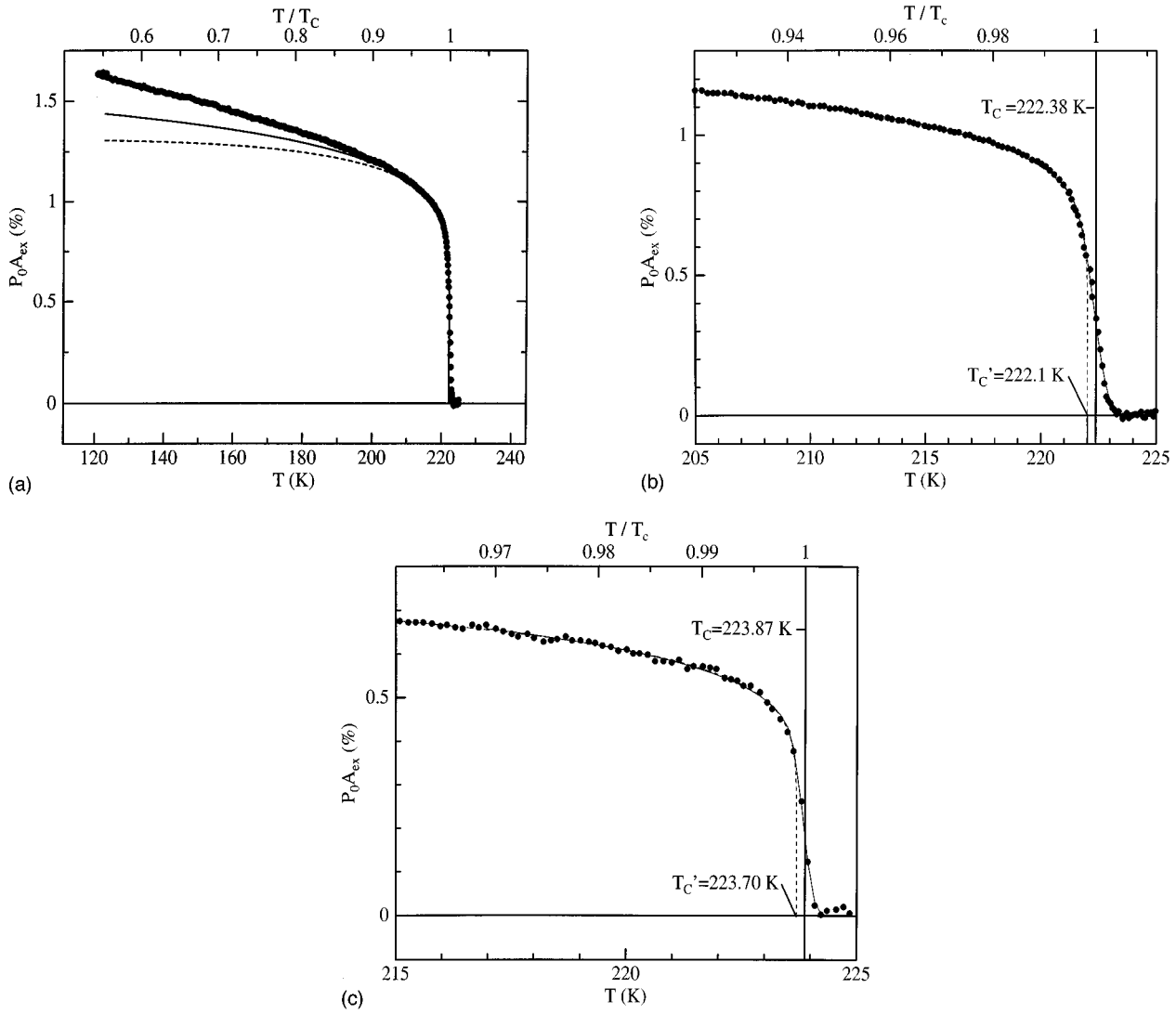

FIG. 7. Exchange asymmetry P_0A_{ex} versus temperature T for two samples with monolayer coverage $\Theta=0.8$. (a) Extended temperature range for sample I; Ising-type power law $P_0A_{ex}=\text{const}(T_C-T)^{1/8}$ (full line) and Onsager solution of the Ising model (broken line) for comparison. (b) Critical range for sample I. Simulation scheme (A) (single T_C) by broken line; simulation scheme (B) (T_C distribution) by full line. Temperature T in absolute units and normalized to T_C, the mean Curie temperature of scheme (B). T_C' is the Curie temperature of scheme (A). (c) as (b), but for sample II. The widths of the distribution, from simulation scheme (B), are given by $\Delta T_C=0.55$ and 0.17 K, the critical exponents by $\beta=(0.133\pm0.002)$ and (0.135 ± 0.003), for samples I and II, respectively.

samples of Fig. 5, with a mean step distance of 40 nm, resulting in $\Delta T_C=0.5$ K. Sample II was prepared on a different W substrate with enhanced step distance which was available only for part of the study, with $\Delta T_C=0.17$ K. It will be shown that the critical exponent β of the magnetization is the same for both samples, in the error limits.

Results for sample I are shown in Figs. 7(a) and 7(b), for sample II in Fig. 7(c), respectively. Figure 7(a) shows P_0A_{ex} versus T for sample I in the whole range of T which was used for measurement. The Onsager solution of the 2D Ising model (broken line) and the corresponding power law with $\beta=1/8$ (full line) are given for comparison. Qualitatively speaking, we note a quite sharp transition. We note further that P_0A_{ex} roughly follows the Onsager solution in a critical range only of about 10%. The fit to the power law is a bit better, as observed in other films in the monolayer regime, too.[21,39] The deviations for lower temperatures may in part be caused by deviations between the temperature dependences of A_{ex} and M, respectively, or they may indicate a true upwards deviation of $M(T)$ from the Ising solution, as a result of finiteness of the anisotropies. The very critical regime of sample I is shown in detail in Fig. 7(b). The usual magnetization tail is now clearly seen. It forms the standard problem for evaluation of data in the critical regime. We used two evaluation schemes. As scheme (A) we used a method which is widely used in experimental work on critical behavior of ultrathin films and has been formulated most clearly by Dürr *et al.*[39] in a paper on Fe films on Au(100). Modifying a recipe given by Suter and Hohenemser,[40] they decided to fit the data by a single power law and to determine the Curie temperature, T_C' in our case, by maximizing the range of $\ln(1-T/T_C')$ over which the data points in a $\ln M$ vs $\ln(1-T/T_C')$ representation form a straight line. The result is shown by the broken line in Fig. 7(b). Data in the tail

above T_C' are discarded for the fit in this scheme. Using a fitting range $0.90 \leqslant T/T_C' \leqslant 0.996$, this scheme formally results in high precision values $T_C' = (222.1 \pm 0.1)$ K and $\beta' = 0.124 \pm 0.001$, the latter being in suggestive agreement with the Ising value $\beta = 1/8$. However, the choice of T_C' and the fitting range remain arbitrary. By varying these fitting parameters, the values of β could be varied roughly between 0.12 and 0.14. To our knowledge, a theoretical foundation of scheme (A) is missing.

However, a quite natural alternative scheme (B) is suggested by Sec. III A, above. Because the sample is composed of a distribution of stripes of variable width and variable values of T_C, we fitted the data alternatively as a convolution of a power law with unique value for β with a Gaussian distribution of Curie temperatures with a mean value T_C and a standard deviation ΔT_C. [A similar scheme was used previously in part of the literature on layered compounds,[41] and for Gd films on W(110) (Ref. 42)]. A fit for $T/T_C > 0.9$, shown in Fig. 7(b) by the full line, results in nonarbitrary parameters $T_C = (222.38 \pm 0.01)$ K, $\Delta T_C = 0.5$ K, and $\beta = (0.133 \pm 0.002)$. Within the statistical error limits, these results are independent of a variation of the only free parameter left, given by the lower limit T_1 of the fitting range, between 0.90 and 0.95 T_C. β switches to even higher values for $T_1 > 0.95\ T_C$. We conclude that the deviation of the critical exponent β from the Ising value $\beta = 1/8$ is significant. The fitting parameter ΔT_C is in excellent agreement with its estimation from the data of Fig. 7 and Eq. (8), $\Delta T_C = 0.55$ K. This confirms our interpretation of the tail as a result of a T_C distribution rather than as a finite-size effect. Scheme (B) therefore has a quite natural foundation in the real structure of our samples, and it avoids the arbitrarities of scheme (A). It contains virtually no arbitrarily parameters of real importance. We conclude that only scheme (B) provides a correct description of our samples and therefore results in the true values for the critical parameters.

The same type of analysis is shown for sample II in Fig. 7(c). The transition is clearly sharper than for sample I [note the different T ranges in Figs. 7(b) and 7(c), respectively]. Apparently, sample II was prepared on a W substrate with exceedingly wide terraces, resulting in a reduced width $\Delta T_C = 0.17$ K of the distribution. The enhanced value of $T_C = 223.87$ K is in accordance with Eq. (6). The resulting value of $\beta = (0.135 \pm 0.003)$ agrees with the value from sample I in the error limits. We take this independence on the width of the tail as a clear confirmation of our scheme (B). We conclude that the mean value $\beta = (0.134 \pm 0.003)$, determined from two samples with strongly different step distances in the *W* substrate, is a well established value of our ferromagnetic monolayer. Its upward deviation from the Ising value $\beta = 0.125$ is significant.

C. Susceptibility

For determining the susceptibility, we used measurements as shown in Fig. 4, for films prepared on the standard substrate of sample I of the last section. Figure 8 shows data for $\Delta A(H)/\Delta H = [A(+H) - A(-H)]/2H$ versus T for a series with various magnetic fields H. As seen from Fig. 4, the data can be interpreted in terms of $\Delta A_{ex}(H)/\Delta H$ above their maxima only. For $T > 223$ K, $\Delta A(H)/\Delta H$ is independent of

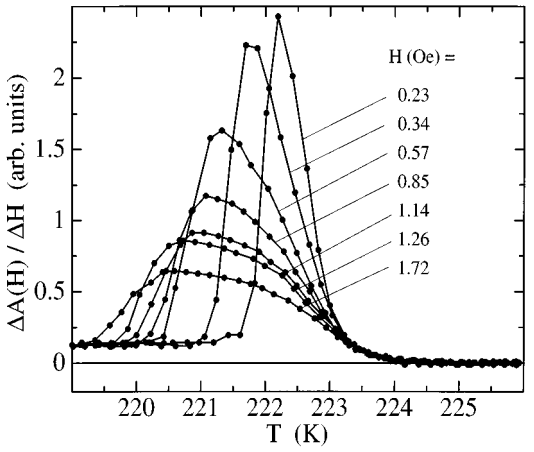

FIG. 8. $\Delta A(H)/\Delta H$ versus T, for different fields H as parameter, for a partial monolayer $\Theta = 0.8$. The data are taken from measurements like in Fig. 4, $\Delta A(H)$ being the difference of both curves after subtracting the constant shift above 225 K, which is caused by beam deflection. The slightly shifted zero level in the ferromagnetic regime is connected with the direct current I_S through the sample (see Fig. 1) which creates the magnetic field and induces a slight change in kinetic energies of the reflected electrons.

H and therefore represents a paramagnetic susceptibility, above T_C. In order to determine a susceptibility in the vicinity of T_C, we replot the data of Fig. 8 in Fig. 9 as isothermal magnetization curves, $P_0 A_{ex}(H)$, for fixed T near T_C (only

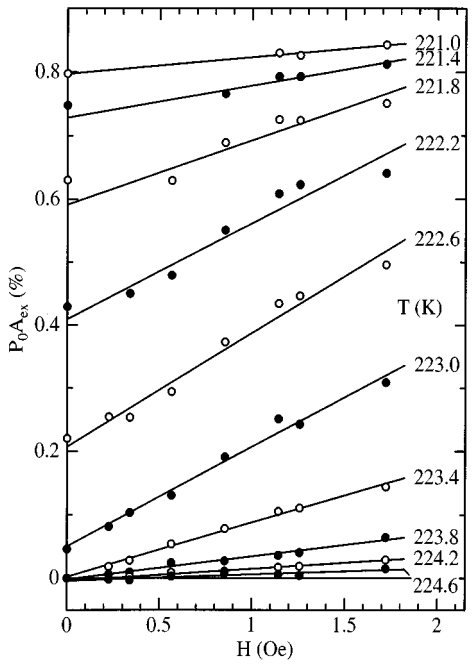

FIG. 9. Exchange asymmetry $P_0 A_{ex}$ versus magnetic field H, for different temperatures T as parameter, for a partial monolayer $\Theta = 0.8$. Data for finite fields were determined from Fig. 8, remanent values for $H = 0$ by separate measurement. Note that the remanent values agree with the linear extrapolation of the finite field values, thus confirming the equivalence of spontaneous and remanent magnetization.

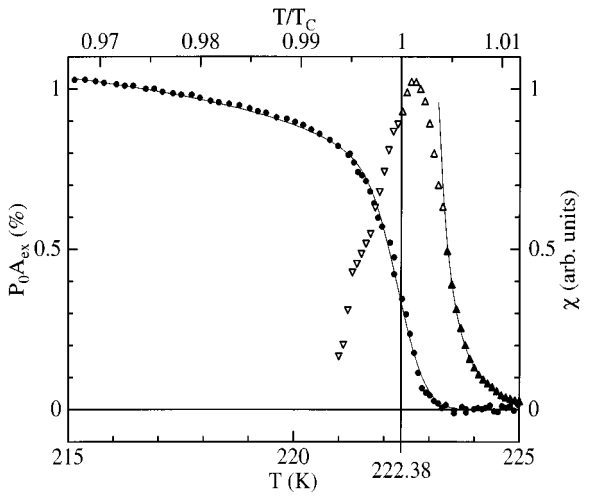

FIG. 10. Magnetic susceptibility χ (triangles) versus T in a linear presentation, in the critical regime, for a partial monolayer $\Theta=0.8$. Full triangles only are used for the power-law fit for $T>T_C$. Exchange asymmetry P_0A_{ex} from Fig. 7(b) for comparison (full circles).

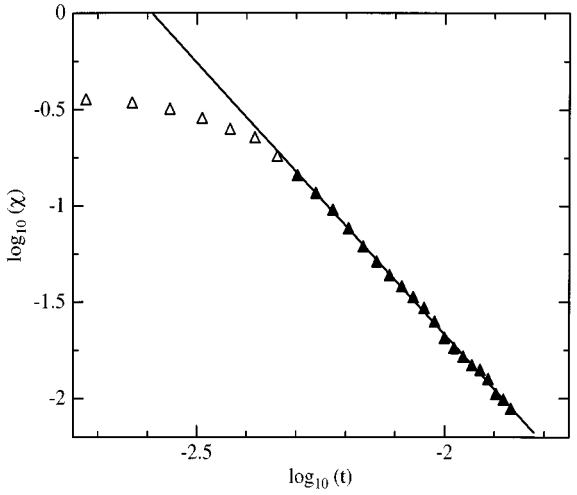

FIG. 11. As Fig. 10, logarithmic presentation of the power-law fit.

data above the maxima in Fig. 8 were used, for which $\Delta A=2A_{ex}$). The remanent value $A_{ex}(0)$, which was measured independently, is included. The figure shows what remains in the critical regime of the square loops, which are expected for lower temperatures: $A_{ex}(H)$ depends linearly on H, with $A_{ex}(0)$ being equal to the value obtained by extrapolation from finite fields. Obviously, $A_{ex}(0)$ represents a spontaneous magnetization, which is identical with the remanent magnetization presented in Sec. III B. The slope represents the susceptibility χ. Accordingly, $P_0A_{ex}(H,T)$, in the critical regime, can be represented by a spontaneous asymmetry $A_{ex,s}=A_{ex}(0,T)$, which is proportional to the spontaneous magnetization M_s, and in a susceptibility $\chi(T)$. The latter is given in Fig. 10 in a linear representation. Remanent values $P_0A_{ex}(0,T)$ from Fig. 7(b) are included for comparison. Note that χ shows its maximum slightly above T_C. This is qualitatively explained from the general observation that the magnetization above T_C reacts more sensitively on the field than below T_C. [For the monolayer case, this phenomenon can be seen most clearly in the magnetometric data of the Ag-covered monolayer W(110)/1Fe(110)/Ag, shown in Ref. 31, Fig. 2). Stated in terms of critical power laws $\chi_+=C_+t^{-\gamma+}$ for $t=(T-T_C)/T_C>0$ and $\chi_-=C_-(-t)^{-\gamma-}$ for $t<0$, respectively, this means $C_+\gg C_-$ [the 2D Ising model predicts $C_+/C_-=37$ (Ref. 43)]. For the present distribution of Curie temperatures, this asymmetry of the amplitudes C_i obviously results in an upwards shift of the maximum of χ. Whereas the data for $T<T_C$ were not sufficient for a power-law fit, such a fit was possible for $T>T_C$. We fitted $\chi_+(T)$ by a single power law, using for T_C the mean value of the distribution from Sec. III B, $T_C=222.38$ K. The fit is shown in Fig. 10 in a linear and in Fig. 11 in a logarithmic presentation. Full symbols only were used for the fit, open symbols not. A single T_C instead of the Gaussian distribution was used in order to avoid integration over the singularities of χ. This does not influence the resulting value of γ because the distance of the used T range from T_C is larger than $4\Delta T_C$, as has been checked numerically using truncated Gaussian distributions which did not overlap with the T range used. The fit results in $\gamma=(2.8\pm0.2)$ (we omit the index + in γ for brevity).

IV. DISCUSSION

The present experimental approach to critical behavior of a ferromagnetic monolayer based on the thermodynamically stable monolayer Fe(110) on W(110) differs from most previous work by several aspects: (a) It is based on a true stable monolayer structure. (b) It is based on quantitative data of the magnetic anisotropies. (c) It is based on a uniaxial sample with an in-plane easy axis, thus avoiding the competition between crystalline and shape anisotropy, which is typical for perpendicularly magnetized films and determines critical parameters. (d) It includes a determination of both the susceptibility and the spontaneous (remanent) magnetization, in the critical regime. (e) Different from our own previous work on the same system, the present work is based on a straightforward model for the magnetization tails, which are explained as a result of distributions in monolayer stripe width, whence of T_C. This interpretation of the tails allowed us to unambiguously determine critical parameters.

The most important result is given by the critical exponents $\beta=(0.134\pm0.003)$ and $\gamma=(2.8\pm0.2)$ which clearly are different from the predictions of the 2D Ising model, $\beta_{Ising}=0.125$ and $\gamma_{Ising}=1.75$, respectively. It is important to note that the same numerical value for β has been obtained for samples I and II [Figs. 7(b) and 7(c)], which differ in the width of the tail by a factor of 3. We conclude that the critical exponents determined above can be taken as independent of the tail width and therefore as properties of the zero tail limiting case as well, that means as properties of the ideal monolayer.

A hint for understanding the enlarged value of γ is contained in a paper of Binder and Landau[9] on the anisotropic Heisenberg model. A key parameter for the critical behavior

is given by the ratio between anisotropy and exchange energies, Δ. The Monte Carlo simulations of Binder and Landau show near $\Delta=0.02$ a crossover from $\gamma=1.75$ for $\Delta>0.02$ to higher effective values for $\Delta<0.02$. For $\Delta=0.01$, an effective value of $\gamma_{\text{eff}}=2.2$ is reported. Note that these effective exponents are not meant as true critical exponents in the sense of the asymptotic approach to T_C, but rather reflect the crossover regime. Our monolayer Fe(110) on W(110) shows uniaxial in-plane anisotropy energies per atom of the order 110 μeV. They are strong in the sense that they are large in comparison with bulk anisotropy energies which are of the order of 4 μeV only. However, they are weak in comparison with the exchange energies, which for bulk Fe are given by $k_B T_C=90$ meV. Hence, Δ is of the order 0.001 and the enhanced value of the effective exponent γ is reasonably explained as a result of the finiteness of the uniaxial anisotropy. However, this explanation does not hold for β, which turns out to be quite insensitive on a reduction of Δ, in the simulations. In our opinion the enlarged value of β rather is related to similar observations in bulk metallic ferromagnets. For example, it has been shown recently in a careful experimental analysis of asymptotic critical behavior of bulk Ni,[44] that the experimental value $\beta_{\text{exp}}=(0.40\pm0.01)$ is definitely larger than the best renormalization-group estimates, $\beta_{\text{RG}}=(0.365\pm0.003)$. Like in our monolayer case, this is an enhancement of the order of 10%, taken there as indicative of long-range interactions. It is argued in Ref. 44 that the effect cannot be explained by the bare magnetostatic interactions, but indicates the presence of long-range exchange interactions in bulk metallic Ni. It remains to be discussed whether in our 2D case magnetostatic interactions are sufficient as an explanation for the enhanced value of β or whether long-range exchange interactions are indicated, too.

In view of the deviation of our critical exponents from the Ising values it is puzzling that Back *et al.*[27] observed just the 2D Ising exponents with high precision in Fe(110) films on W(110), prepared at 300 K, which show a Curie temperature slightly above 300 K and consist of roughly 1.5 monolayers. Films with this value of T_C, between the Curie temperatures T_C (ML)=230 K of the monolayer and T_C (DL)=450 K (Ref. 28) of the double layer, have been shown to consist of weakly coupled single-domain ferromagnetic double-layer islands on a monolayer substrate.[28] The films of Back *et al.*[27] therefore are definitely not true monolayer structures. In our opinion, the agreement with the 2D Ising model must be interpreted in terms of supermagnetism[45] as follows. The 2D Ising model is concerned with a regular 2D arrangement of coupled entities with infinite uniaxial anisotropy. We guess that those entities are the double-layer islands of Back's sample. Having areas of the order of some 100 nm^2, they consist of roughly 10 000 atoms, and their total anisotropy is enhanced from the atomic anisotropy energy of the order of $10^{-3}\ k_B T_C$ to an island value of $10\ k_B T_C$, roughly. Apparently, it is this strong anisotropy only, irrespective of a regularity of size or of arrangement of the entities, which is responsible for $\beta=1/8$. It is a challenge for theory to show whether this Ising exponent is actually a property of such a 2D arrangement of coupled uniaxial islands with virtually infinite anisotropy, independent of whether they are arranged in a regular or in an irregular manner.

In conclusion, we have experimentally investigated the critical behavior of the thermodynamically stable pseudomorphic monolayer Fe(110) on W(110), which shows uniaxial magnetic anisotropy with the easy axis in the plane. The critical behavior can be interpreted in terms of a 2D anisotropic Heisenberg model. We found small but definite deviations of critical exponents $\beta=(0.134\pm0.003)$ and $\gamma=(2.8\pm0.2)$ from their 2D Ising values $\beta=0.125$ and $\gamma=1.75$, respectively. The enhanced value of γ can be explained from the fact that the anisotropy energies per atom are small in comparison with exchange coupling energies. The enhanced value of β is indicative of long-range interactions.

ACKNOWLEDGMENTS

We thank K. Binder for fruitful discussions and for a critical reading of the manuscript. This work was supported by the Deutsche Forschungsgemeinschaft.

*Corresponding author. FAX+49-5323-72-3600. Electronic address: gradmann@physik.tu-clausthal.de

[1] L. Onsager, Phys. Rev. **65**, 117 (1944).
[2] C. N. Yang, Phys. Rev. **85**, 808 (1952).
[3] N. D. Mermin and H. Wagner, Phys. Rev. Lett. **17**, 1133 (1966).
[4] R. B. Griffiths, Phys. Rev. Lett. **24**, 176 (1970).
[5] K. G. Wilson, Phys. Rev. B **4**, 3174 (1971).
[6] V. L. Berezinskii, Sov. Phys. JETP **32**, 493 (1971).
[7] J. M. Kosterlitz and D. J. Thouless, J. Phys. C **6**, 1181 (1973).
[8] S. T. Bramwell and P. C. W. Holdsworth, J. Appl. Phys. **73**, 6096 (1993).
[9] K. Binder and D. P. Landau, Phys. Rev. B **13**, 1140 (1976).
[10] M. Bander and D. L. Mills, Phys. Rev. B **38**, 12 015 (1988).
[11] A. Abanov, V. Kalatsky, V. L. Pokrovsky, and W. M. Saslow, Phys. Rev. B **51**, 1023 (1995).
[12] R. J. Birgeneau, J. Skalyo, and G. Shirane, J. Appl. Phys. **41**, 1303 (1970).
[13] L. J. de Jongh and A. R. Miedema, Adv. Phys. **23**, 1 (1974).
[14] U. Gradmann, in *Handbook of Magnetic Materials*, edited by K. H. J. Buschow (Elsevier Science, Amsterdam, 1993), Vol. 7/1, pp. 1–96.
[15] J. A. C. Bland and B. Heinrich, *Ultrathin Magnetic Structures* (Springer, Berlin, 1994), Vols. I and II.
[16] J. Thomassen, F. May, B. Feldmann, M. Wuttig, and H. Ibach, Phys. Rev. Lett. **69**, 3831 (1992).
[17] C. Liu and S. D. Bader, J. Appl. Phys. **67**, 5758 (1990).
[18] Z. Q. Qiu, J. Pearson, and S. D. Bader, Phys. Rev. B **49**, 8797 (1994).
[19] D. P. Landau, Phys. Rev. B **13**, 129 (1976).
[20] E. V. Albano, K. Binder, D. W. Heermann, and W. Paus, Z. Phys. B **77**, 445 (1989).
[21] Z. Q. Qiu, J. Pearson, and S. D. Bader, Phys. Rev. Lett. **67**, 1646 (1991).
[22] Y. Li and K. Baberschke, Phys. Rev. Lett. **68**, 1208 (1992).
[23] U. Gradmann, M. Przybylski, H. J. Elmers, and G. Liu, Appl. Phys. A **49**, 563 (1989).
[24] U. Gradmann and G. Waller, Surf. Sci. **116**, 539 (1982).
[25] C. H. Back, C. Würsch, D. Kerkmann, and D. Pescia, Z. Phys. B **96**, 1 (1994).
[26] C. H. Back, C. Würsch, and D. Pescia, Z. Phys. B **98**, 69 (1995).
[27] C. H. Back, C. Würsch, A. Vaterlaus, U. Ramsperger, U. Maier,

and D. Pescia, Nature (London) **378**, 597 (1995).
[28] H. J. Elmers, J. Hauschild, H. Fritzsche, G. Liu, U. Gradmann, and U. Köhler, Phys. Rev. Lett. **75**, 2031 (1995).
[29] M. Przybylski and U. Gradmann, Phys. Rev. Lett. **59**, 1152 (1987).
[30] M. Przybylski and U. Gradmann, J. Phys. (Paris) Colloq. **49**, C8-1705 (1988).
[31] H. J. Elmers, G. Liu, and U. Gradmann, Phys. Rev. Lett. **63**, 566 (1989).
[32] H. J. Elmers, J. Hauschild, H. Höche, U. Gradmann, H. Bethge, D. Heuer, and U. Köhler, Phys. Rev. Lett. **73**, 898 (1994).
[33] H. J. Elmers, J. Hauschild, G. Liu, and U. Gradmann, J. Appl. Phys. **79**, 4984 (1996).
[34] H. J. Elmers, J. Hauschild, and U. Gradmann, J. Magn. Magn. Mater. **140-144**, 671 (1995).
[35] H. J. Elmers, J. Hauschild, and U. Gradmann, J. Magn. Magn. Mater. **140-144**, 1559 (1995).
[36] H. J. Elmers, Int. J. Mod. Phys. **9**, 3115 (1995).
[37] R. Feder and H. Pleyer, Surf. Sci. **117**, 285 (1982).
[38] J. Kohlhepp, H. J. Elmers, S. Cordes, and U. Gradmann, Phys. Rev. B **45**, 12 287 (1992).
[39] W. Dürr, M. Taborelli, O. Paul, R. Germar, W. Gudat, D. Pescia, and M. Landolt, Phys. Rev. Lett. **62**, 206 (1989).
[40] R. M. Suter and C. Hohenemser, J. Appl. Phys. **50**, 1814 (1979).
[41] R. J. Birgeneau, J. Als-Nielsen, and G. Shirane, Phys. Rev. B **16**, 280 (1977).
[42] U. Stetter, M. Farle, K. Baberschke, and W. G. Clark, Phys. Rev. B **45**, 503 (1992).
[43] J. W. Essam and M. E. Fisher, J. Chem. Phys. **38**, 802 (1963).
[44] M. Seeger, S. N. Kaul, H. Kronmüller, and R. Reisser, Phys. Rev. B **51**, 12 585 (1995).
[45] S. Morup, M. B. Madsen, J. Franck, J. Villadsen, and C. J. W. Koch, J. Magn. Magn. Mater. **40**, 163 (1983).